



Synthesis and synergistic studies of isatin based mixed ligand complexes as potential antifungal therapeutic agents



Ovas Ahmad Dar^a, Shabir Ahmad Lone^b, Manzoor Ahmad Malik^a, Faisal Mohammed Aqlan^c, Mohmmad Younus Wani^c, Athar Adil Hashmi^{a,*}, Aijaz Ahmad^{b,d,**}

^a Department of Chemistry, Jamia Millia Islamia, New Delhi 110025, India

^b Clinical Microbiology and Infectious Diseases, School of Pathology, Faculty of Health Sciences, University of the Witwatersrand, Johannesburg, 2193, South Africa

^c Chemistry Department, Faculty of Science, University of Jeddah, P.O. Box 80327, Jeddah 21589, Kingdom of Saudi Arabia

^d Infection Control, Charlotte Maxeke Johannesburg Academic Hospital, National Health Laboratory Service, Johannesburg, 2193, South Africa

ARTICLE INFO

Keywords:

Inorganic chemistry
Organic chemistry
Pharmaceutical chemistry
Microbiology
Pharmaceutical science

ABSTRACT

Metal based drugs are important class of chemotherapeutic agents that have the potential to circumvent drug resistance. Increasing drug resistance, treatment failures and limited treatment options necessitates the development of new therapeutic drugs with different mechanisms of action. Towards this direction, we synthesized a series of isatin based mixed ligand complexes of [Cu(dbm)LClH₂O] (**m1c1**), [Co(dbm)LCl₂]⁻ (**m1c2**) and [Ni(dbm)LClH₂O] (**m1c3**) and evaluated their antifungal activity alone and in combination with fluconazole (FLC) against seven different *Candida albicans* isolates. The insight mechanism of antifungal action was revealed by studying apoptosis via terminal deoxynucleotidyl transferase dUTP nick-end labeling (TUNEL) assay. The study revealed that all these compounds showed antifungal activity at varying concentrations with **m1c3** as the most potent compound with minimum inhibitory concentration ranging from 0.5–8 µg/mL and minimum fungicidal concentration ranging from 4–16 µg/mL. Upon combination with FLC, most of the interactions were either synergistic (54 %) or additive (32 %) with no antagonistic combination against any of the tested isolate. The study on their mechanism of action revealed that these compounds show apoptotic effect on *C. albicans* at sub-inhibitory concentrations, suggesting that strategies to target this process may augment the current antifungal treatment modalities.

1. Introduction

Fungal infections take more than 1.3 million lives each year worldwide, nearly as many as tuberculosis. There is an urgent need for the development of new antifungal agents or strategies that could add to the current armament against fungi and augment the treatment options which have been challenged by increasing multi-drug resistance. A good strategy to design new antifungal drugs has been the complexation of bioactive compounds with transition metals. Metal complexes of sulfonamide drugs, fluoro quinolones and penicillin have already been synthesized and it was observed that metalation enhances the efficacy of the already established drugs [1, 2, 3]. Pd(II) complex of tetracycline has been reported to have potency sixteen times more than the parent compound against *E.coli* HB101/pBR322, a bacterial strain resistant to tetracycline whereas Pd(II) complex of doxycycline is two times more

potent than doxycycline against resistant strain [2]. In another study Copper(II) norfloxacin complex sharply decreased the viability and proliferation rate of HL-60 cells, leading to cell death through apoptosis in a time-dependent manner [1].

Isatin possess an indole ring structure, common to many pharmaceuticals and heterocyclic natural products of biological interest [4]. Its derivatives have shown important biological activities such as antimicrobial, anticonvulsant, cysticidal, antimalarial, herbicidal, antimycobacterial, anticancer, anti-inflammatory and antiviral [5, 6]. They also exhibit anti-HIV, antihelminthic and antiprotozoal activities [7]. Dibenzoylmethane (DBM) on the other hand belongs to a small group of flavonoids known as β-hydroxychalcones [8] and is rarely found in nature. DBM and its derivatives have attracted considerable attention because of their promising biological activities [9, 10]. DBM has also been found as a possible candidate for dementia treatment [11]. Based on

* Corresponding author.

** Corresponding author.

E-mail addresses: aah_ch@yahoo.co.in (A.A. Hashmi), aijaz.ahmad@wits.ac.za (A. Ahmad).

our previous studies it is our premise that complexation of bioactive ligands with transition metals and combination therapy greatly improves the treatment efficacy and provides a broader treatment window that greatly helps to circumvent drug resistance [12, 13, 14]. In this study, we proposed to prepare some mixed ligand complexes of a ligand derived from isatin and DBM as a co-ligand and tested them against different FLC susceptible and resistant *C. albicans* isolates alone and in combination with FLC to obtain new antifungal agents or potentiators that could be used in combination therapy. The mechanism of action was studied by TUNEL assay.

2. Results and discussion

The mixed ligand metal complexes (**mlc1-mlc3**) were successfully synthesized by reacting equimolar amounts of Schiff base ligand (**L**) with the corresponding metal salts and dibenzoylmethane in presence of NaOH as shown in [Scheme 1](#). The synthesized metal complexes were colored, air stable and insoluble in most of the organic solvents except DMF and DMSO. The ligand (**L**) and metal complexes (**mlc1-mlc3**) were analyzed using various physico-chemical properties like melting point, yield, color, elemental analysis and conductivity measurements. The data is shown in [Table 1](#). It was concluded from the results that **mlc1** and **mlc3** complexes had molar conductance values of the 21.25 and 24.72 $\Omega^{-1}\text{cm}^2\text{mol}^{-1}$ respectively, indicating their non-electrolytic nature. While **mlc2** complex had the molar conductance of 86.43 $\Omega^{-1}\text{cm}^2\text{mol}^{-1}$ indicated the electrolytic nature of this complex. All the compounds were further characterized by various spectral techniques like FT-IR, NMR, UV-Vis spectra, mass spectrometry, magnetic moments and thermal studies. The analytical data of the ligand and metal complexes are in good

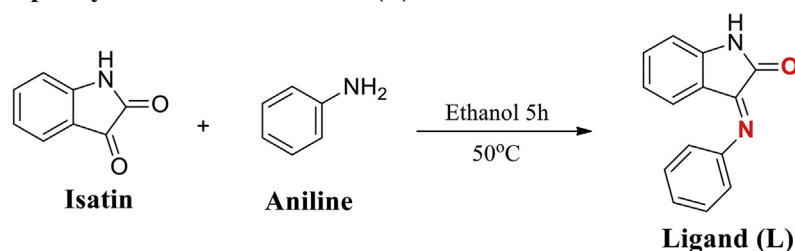
agreement with their proposed formula.

2.1. FT-IR spectral studies

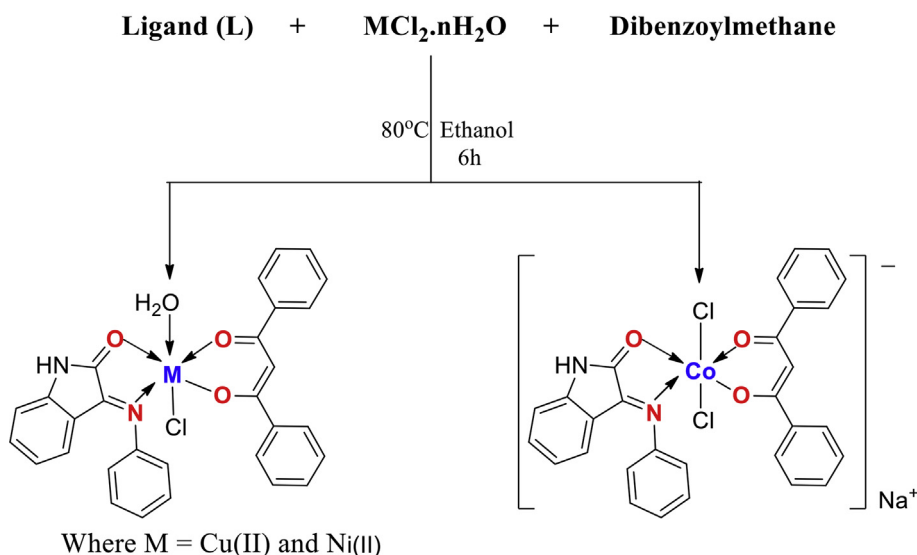
The infrared spectrum of the synthesized Schiff base ligand and metal complexes were taken in the range of 4500–400 cm^{-1} to interpret the nature of the ligands to metal ion bonding. Upon chelation the intensities of the peaks are expected to change as compared to that of the ligands and also some new peaks appeared due to chelation. The IR spectra of the Schiff base ligand, DBM and **mlc1** metal complex as an example is shown in [Fig. 1](#).

The IR spectrum of the ligand (**L**) displayed a strong band at 1600 cm^{-1} corresponding to $\nu(\text{C}=\text{N})$ of imine group. In complexes (**mlc1-mlc3**) the imine $\nu(\text{C}=\text{N})$ of the ligand shifted to lower wavenumbers 1543–1586 cm^{-1} upon coordination to metal [15]. A broad band of medium intensity at 3130–3205 cm^{-1} assigned to $\nu(\text{N}-\text{H})$ was also observed. The strong band observed in the ligand at 1727 cm^{-1} is characteristic of $\nu(\text{C}=\text{O})$ amide [5]. In complexes this band was shifted to lower frequencies (10–12 cm^{-1}), indicating the coordination of carbonyl oxygen of the ligand to metal ions. In DBM the band present at 1665 cm^{-1} correspond to $\nu(\text{C}=\text{O})$ and in complexes this band is shifted to lower frequencies signifying the coordination of carbonyl oxygen of DBM to metal ions [16]. In DBM the band present at 1282 cm^{-1} was assigned to the phenolic C–O stretching mode. In case of complexes (**mlc1-mlc3**) this band was found at higher wavenumbers in the range of 1287–1290 cm^{-1} confirming the involvement of the enolic oxygen in coordination. The **mlc1** and **mlc3** complexes show a broad band at 3500 and 3468 cm^{-1} characteristic of $\nu(\text{OH})$ coordinated water molecule. The IR spectra of the **mlc2** and **mlc3** complexes are shown in supplementary data.

Step 1 Synthesis of Schiff base (L)



Step 2 Synthesis of mixed ligand complexes (C1-C3)



Scheme 1. Synthesis of isatin based ligand (L) and mixed ligand complexes (mlc1-mlc3).

Table 1
Physico-chemical properties of Ligand (L) and complexes (**mlc1-mlc3**).

Comp.	Colour	Mol. formula	Mol. Wt.	(m/z) ratio	Yield (%)	Λ_m ($\Omega^{-1} \text{ cm}^2 \text{ mol}^{-1}$)	Mp ($^{\circ}\text{C}$)	μ_{eff} (BM)
L	Orange	$\text{C}_{14}\text{H}_{10}\text{N}_2\text{O}$	222.2	223.0	80	-	162	-
mlc1	Yellow Green	$[\text{C}_{29}\text{H}_{23}\text{ClCuN}_2\text{O}_4]$	562.5	563.5	70	21.25	272	1.85
mlc2	Brown	$[(\text{C}_{29}\text{H}_{21}\text{Cl}_2\text{CoN}_2\text{O}_3)\text{Na}]$	598.3	599.2	68	86.43	221	4.60
mlc3	Reddish Brown	$[\text{C}_{29}\text{H}_{23}\text{Cl N}_2\text{NiO}_4]$	557.6	558.7	72	24.72	215	3.10

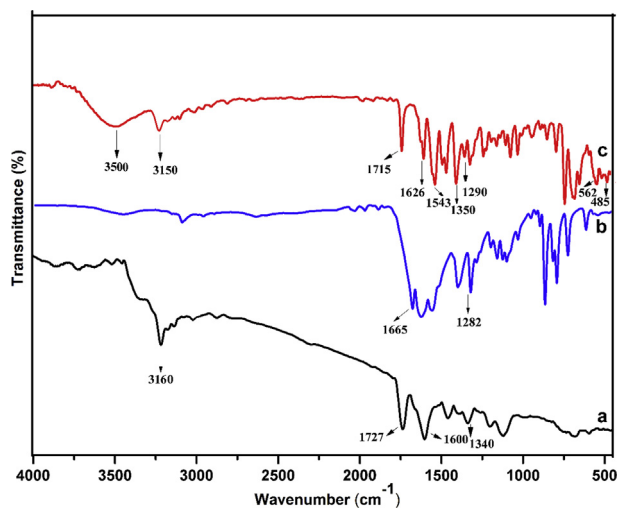


Fig. 1. FT-IR spectra of (a) ligand (L), (b) DBM and (c) mlc1 complex.

The low frequency region of the spectra in complexes (**mlc1-mlc3**) showed the presence of new medium and weak intensity bands in the region of $400\text{--}600\text{cm}^{-1}$, assigned to $\nu(\text{M-O})$ and $\nu(\text{M-N})$ stretching vibrations. The above results revealed that the two ligands coordinated to metal ions via the carbonyl oxygen of dibenzoylmethane moiety in enolic or ketonic form and the azomethine nitrogen and carbonyl oxygen of ligand (L).

2.2. Mass spectrometry

The mass spectra of the ligand (L) and metal complexes (**mlc1-mlc3**) were recorded and were found in close agreement with the molecular weights of these compounds. The mass spectra $[\text{M} + \text{H}]^+$ of the ligand showed the molecular ion peak at m/z 223.0 and the mixed ligand complexes (**mlc1-mlc3**) showed molecular ion peaks at 563.5, 599.2 and 558.7 respectively. The mass spectrum is given in supplementary data.

2.3. Magnetic susceptibility and electronic spectral studies

The electronic spectra were recorded in 10^{-3}M DMSO solution in the range of $200\text{--}800\text{ nm}$ at room temperature using same solvent as blank. Two bands were observed in the ligand at 255 and 305 nm. The first band appearing at 255 nm is attributed to $\pi\text{-}\pi^*$ transitions of the aromatic rings and the band at 305 nm might be attributed to the $n\text{-}\pi^*$ transitions of the azomethine group. In complexes the $n\text{-}\pi^*$ transition band is observed in the range of $300\text{--}360\text{ nm}$. In complexes this band undergoes shift due to the coordination of azomethine nitrogen with the metal ions as shown in **Fig. 2**. The complex (**mlc1**) displayed the broad asymmetric band in the range of $505\text{--}638\text{ nm}$ due to the combination of three bands ${}^2\text{B}_{1g} \rightarrow {}^2\text{A}_{1g}$ (ν_1), ${}^2\text{B}_{1g} \rightarrow {}^2\text{B}_{2g}$ (ν_2) and ${}^2\text{B}_{1g} \rightarrow {}^2\text{E}_g$ (ν_3) which are similar in energy. The broadness of the band revealed its distortion from the octahedral geometry. The magnetic moment of **mlc1** was found to be 1.85 B.M, which is an indicative of an octahedral geometry. In complex (**mlc2**) the high intensity band at 420 nm may be assigned as the $\text{L} \rightarrow \text{M}$ charge transfer transition. In this complex the low intense bands at 492 and 605 nm corresponds to ${}^4\text{T}_{1g}(\text{F}) \rightarrow {}^4\text{T}_{2g}(\text{P})$ and ${}^4\text{T}_{1g}(\text{F}) \rightarrow {}^4\text{A}_{2g}(\text{F})$ excitations

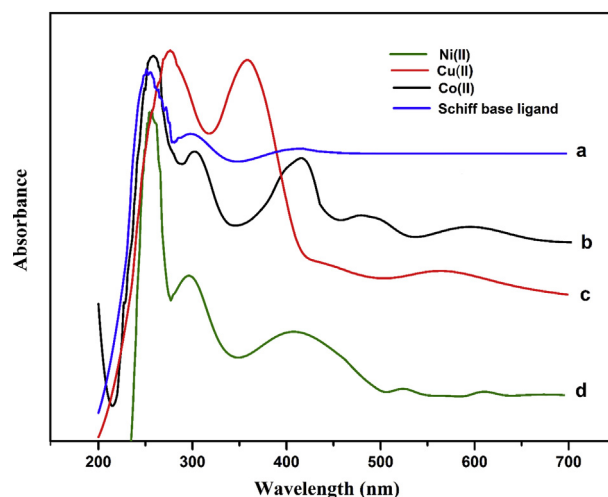


Fig. 2. UV-Vis spectra of (a) ligand (L), (b) mlc2, (c) mlc1 and (d) mlc3 complexes in 10^{-3} M DMSO solution.

respectively [17]. The magnetic moment of **mlc2** was found to be 4.6 B.M. The magnetic moment and electronic spectral data suggest an octahedral geometry around the Co(II) ion. The complex (**mlc3**) exhibited bands at 425, 525 and 620 nm corresponding to three spin allowed transitions as ${}^3\text{A}_{2g}(\text{F}) \rightarrow {}^3\text{T}_{1g}(\text{P})$, ${}^3\text{A}_{2g}(\text{F}) \rightarrow {}^3\text{T}_{1g}(\text{F})$ and ${}^3\text{A}_{2g}(\text{F}) \rightarrow {}^3\text{T}_{2g}(\text{F})$ respectively. The magnetic moment for **mlc3** was found to be 3.1 B.M. The electronic spectra and magnetic moment suggest an octahedral geometry around the Ni(II) ion [15].

2.4. ${}^1\text{H}$ NMR and ${}^{13}\text{C}$ NMR spectra

The ${}^1\text{H}$ NMR of the ligand (L) and complexes (**mlc1-mlc3**) was recorded in CDCl_3 and DMSO- d_6 respectively using tetramethylsilane (TMS) as internal standard. The ${}^1\text{H}$ NMR of the ligand (L) gave characteristic signal at 9.46 ppm (s, 1H) which was assigned to the NH proton [17]. In addition, the aromatic protons of the ligand appeared as multiplets in the range of 6.65–7.49 ppm (m, 9H). The ${}^1\text{H}$ NMR of the complexes (**mlc1-mlc3**) was not clear probably due to the paramagnetic nature of the complexes. The ${}^1\text{H}$ NMR and ${}^{13}\text{C}$ NMR of the ligand and complexes obtained as such is given in the supporting information (see Figs. S7-S14).

2.5. Thermogravimetric studies (TG and DTG)

The thermal analysis of the complexes was studied by using thermogravimetric techniques within a temperature range from room temperature to $1000\text{ }^{\circ}\text{C}$ at a heating rate of $10\text{ }^{\circ}\text{C}/\text{min}$. As a representative case the TG/DTG curve of complex **mlc3** is depicted in **Fig. 3**. The temperature intervals and the percentage loss of masses of complexes is summarized in **Table 2**. The thermal decomposition of the complexes **mlc1-mlc3** undergoes in three stages. The first stage is a degradation step where weight loss of 3% (Calcd. 3.2%) in the temperature range of $50\text{--}200\text{ }^{\circ}\text{C}$ with DTG peaks at $120\text{ }^{\circ}\text{C}$ was observed in **mlc1** complex. This weight loss is due to the liberation of one coordinated water. The **mlc1** complex in the second stage degrades at the temperature range of $200\text{--}400\text{ }^{\circ}\text{C}$ by

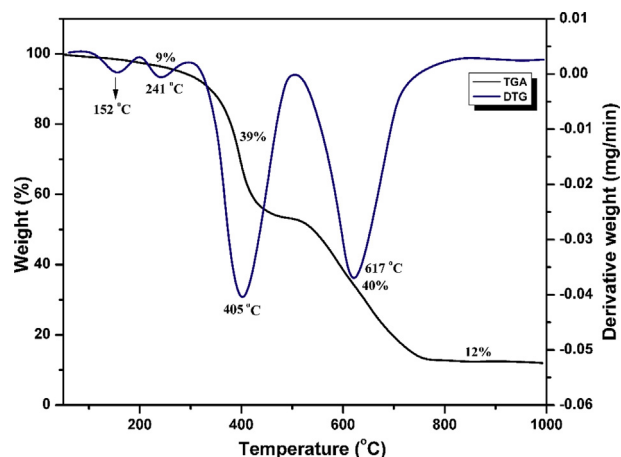


Fig. 3. TGA and DTG curves of mlc3 complex.

the simultaneous loss of coordinated chlorine atom and $C_{14}H_{10}N_2O$ moiety with the weight loss of 45% (Calcd. 45.8%) with DTG peaks observed at 210 and 396 °C. The third stage of decomposition in this complex occurred at the temperature range of 400–700 °C with the weight loss of 39% (Calcd. 39.7%) due to the loss of $C_{15}H_{12}O_2$ fragment with DTG peak observed at 590 °C. The overall weight loss observed in this complex was found to be 87% (Calcd. 88.7%). The metallic residue left has the observed weight of 13% (Calcd. 11.3%).

The **mlc2** complex undergoes decomposition in three stages. The first stage occurred at the temperature range of 100–270 °C with the weight loss of 12% (Calcd. 12.28%). This weight loss corresponds to the loss of Cl_2 molecule with DTG peak observed at 242 °C. The second stage of degradation occurred at the temperature range of 270–590 °C with the weight loss of 38% (calcd. 38.49%). This weight loss corresponds to the loss of $C_{14}H_{10}N_2O$ fragment with DTG peaks observed at 378 °C. The third stage in this complex proceeded with one degradation step. This degradation step occurred within the temperature range of 590–860 °C with the weight loss of 39% (Calcd. 39.84%), which corresponds to the loss of $C_{15}H_{12}O_2$ fragment with DTG peak observed at 700 °C. The total weight loss observed was found to be 89% as against the calculated value of 89.61%. The metallic residue finally left has the observed mass of 11% as against the calculated value of 10.39%.

In **mlc3** complex the first stage of degradation occurred at the temperature range of 100–300 °C with the weight loss of 9% (calcd. 9.5%). This weight loss corresponds to the simultaneous loss of one coordinated water molecule and one coordinated chlorine atom. The DTG peaks were observed at 152 and 241 °C. The second stage of degradation occurred at the temperature range of 300–515 °C with the weight loss of 39% (calcd. 39.77%). This weight loss corresponds to the loss of $C_{14}H_{10}N_2O$ fragment with DTG peaks observed at 405 °C. The third stage proceeded with one degradation step and occurred within the temperature range of 590–860

Table 2
Thermoanalytical results (TG and DTG) of mixed ligand metal complexes.

Complex	TG range(°C)	DTG _{max} (°C)	n*	Found (calcd. %)		Assignment	Metallic residue
				Mass loss	Total mass loss		
[C ₂₉ H ₂₃ ClCuN ₂ O ₄]	50–200	120	1	3.0(3.2)		Loss of one coordinated H ₂ O molecule	Cu
	200–500	310,390	2	45(45.8)	87(88.7)	Loss of $\frac{1}{2}Cl_2$ and $C_{14}H_{10}N_2O$	
[(C ₂₉ H ₂₁ Cl ₂ CoN ₂ O ₃)/Na]	500–800	590	1	39(39.7)		Loss of $C_{15}H_{12}O_2$	Co
	100–270	242	1	12(12.28)		Loss of coordinated Cl_2 molecule	
	270–590	378	1	38(38.49)	89(89.61)	Loss of $C_{14}H_{10}N_2O$	
	590–860	700	1	39(38.84)		Loss of $C_{15}H_{12}O_2$	
[C ₂₉ H ₂₃ Cl N ₂ NiO ₄]	100–300	152,241	2	9(9.5)		Loss of one coordinated H ₂ O and $\frac{1}{2}Cl_2$ molecule	Ni
	300–515	405	1	39(39.77)	88(89.39)	Loss of and $C_{14}H_{10}N_2O$	
	515–765	617	1	40(40.12)		Loss of $C_{15}H_{12}O_2$	

n* = number of decomposition.

°C with the weight loss of 40% (Calcd. 40.12%), which corresponds to the loss of $C_{15}H_{12}O_2$ fragment with DTG peak observed at 617 °C. The total weight loss observed was found to be 88% as against the calculated value of 89.39%. The metallic residue finally left has the observed mass of 12% as against the calculated value of 10.61%.

From all the physical measurements and spectroscopic techniques, the metal complex **mlc1** appears to have a distorted octahedral geometry and the complexes **mlc2** and **mlc3** have octahedral geometry. The structures of these complexes was drawn in chemdraw ultra 12.0 and energy minimized (MM2) in chem3D pro using the set functions. The energy minimized structures are shown in Fig. 4.

2.6. Biological studies

2.6.1. Minimum inhibitory concentrations and minimum fungicidal concentrations

The ligand (**L**) and its mixed ligand complexes (**mlc1-mlc3**) were evaluated *in vitro* against seven different isolates of *C. albicans* by microbroth dilution assay. All the MIC and MFC results are summarized in Table 3. The MIC values range from 0.5 µg/mL to 500 µg/mL while as MFC values vary from 4 µg/mL to 1000 µg/mL. The complex **mlc3** exerted highest inhibitory activity against all the tested fungal isolates with an MIC values ranging from 0.5 – 8 µg/mL while as the ligand has shown the least inhibitory activity ranging from 125 – 500 µg/mL. We did not evaluate dibenzoylmethane (DBM) because it is known to be inactive. As a positive control, FLC was used because of its common use in the treatment *Candida* infections. As expected, the MIC values for FLC against susceptible and standard laboratory strain was ranging from 0.12 µg/mL to 0.25 µg/mL while as these values range from 16 µg/mL to 32 µg/mL against FLC resistant isolates. These results are congruent with the CLSI Interpretive Guidelines for *In vitro* Susceptibility Testing of *Candida* species [18]. Furthermore, all the test compounds were prepared to different concentrations using 1% DMSO and therefore DMSO was used as negative vehicle control and was observed to have no inhibitory activity against any of the tested isolates. Based on the MIC results, order of potency of these compounds was **mlc3**>**mlc2**>**mlc1**>**L**. The MIC data revealed that the structural changes from ligand to its metal complexes produced the marked enhancement in their potency as antifungal agents. Unlike FLC, all the test compounds showed MFC values indicating their potential to kill the fungal pathogen within varying concentration ranges.

2.6.2. In vitro combination antifungal activities

Having established the individual MIC values for **L**, **mlc1**, **mlc2**, **mlc3** and **FLC**, the MIC and FICI values of these compounds in combination with the FLC were determined in 1:1 combination by microbroth dilution assay against seven *C. albicans* isolates (See supporting information Table S1). When combined with FLC (n = 28), most of the combinations were either synergistic (54%; n = 15) or additive (32%; n = 9) and only few were indifferent (14%; n = 4) with no antagonistic interaction. Ligand (**L**) when combined with FLC showed strong synergistic/inhibitory

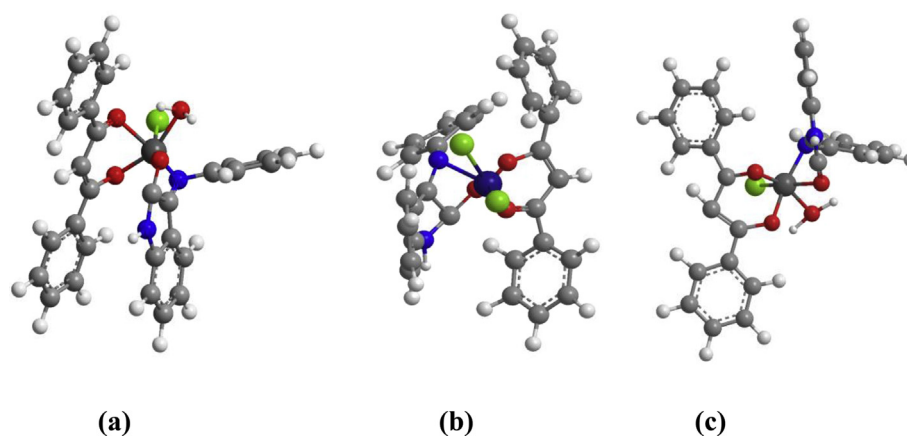


Fig. 4. Energy minimized (MM2) structures of (a) mlc1, (b) mlc2 and (c) mlc3 complexes.

Table 3

Minimum inhibitory concentrations ($\mu\text{g}/\text{mL}$) of ligand (L) and mixed ligand complexes (**mlc1-mlc3**) against FLC susceptible and resistant isolates.

Isolates		Ligand (L)		mlc1		mlc2		mlc3		FLC
		MIC	MFC	MIC	MFC	MIC	MFC	MIC	MFC	MIC
Lab strain	<i>C. albicans</i> SC5314	125	500	125	250	32	125	0.5	8	0.25
FLC Susceptible strains	4175	250	500	250	500	64	500	2	8	0.12
	4179	250	1000	125	500	64	125	1	4	0.25
	4180	125	500	125	500	64	125	1	4	0.25
FLC Resistant strains	4085	500	1000	250	500	125	500	8	16	16
	4122	500	1000	250	500	125	500	4	8	32
	4135	500	1000	250	500	125	500	8	16	32

effects against the majority of the tested *C. albicans* strains (6 out of 7) with FICI values ranging from 0.146–0.380 (See supporting information Table S1). Likewise, the combination of **mlc1** with FLC also exhibited good synergy against the majority of the tested *C. albicans* strains (5 out of 7), with FICI values ranging from 0.266–0.500. Interestingly, **mlc3** which was the most active compound showed only one synergistic activity against one of the resistant isolates while as all other activities are either additive or indifferent. Similar findings were reported by Shrestha *et al.*, where they found less potent amphiphilic tobramycin analogue C_{12} showing more synergistic inhibitory effects when combined with azoles against all strains of *C. albicans* than its another analogue C_{14} [19]. A comparison between FLC susceptible and FLC resistant isolates indicated that resistant isolates showed more synergy (75%; $n = 12$) than susceptible isolates (50%; $n = 12$), which are congruent with our previous findings [13, 14, 20]. Despite only 54% combinations were synergistic, it is important to mention that the MIC values of FLC were greatly reduced when used with test compounds against all the tested fungal strains. These findings set up the base for further studies to use these and similar compounds as chemosensitizing agents with FLC to provide a new strategy to fight fungal infections caused by resistant strains.

2.6.3. TUNEL assay: FITC labeling

Numerous molecular level apoptotic regulators have been identified and characterized [21]. DNA damage is a well-established hallmark of late apoptosis. TUNEL assay was used as primary screening tool for apoptosis as it targets fundamental apoptotic event in yeast cells. To investigate whether the newly synthesized compounds display features of the late stages of apoptosis in *C. albicans*, we evaluated DNA fragmentation and visualized it with the help of a TUNEL assay by labeling 3'-OH ends of nicked DNA with fluorescent dUTP (TUNEL-FITC). Fig. 5 represents *C. albicans* cells (SC5314) exposed to MIC and $\frac{1}{2}$ MIC values of **mlc3** for 1 h, exhibiting a significant amount of changes in nuclear DNA and that of the ligand (L) and complexes **mlc1** and **mlc2** are shown in Fig. S17. In cells exposed to low concentrations of the test compounds

(MIC/2), the proportion of TUNEL-positive nuclei (green fluorescence) was significantly increased compared to that of the untreated control population. The analyses of results revealed remarkable apoptosis for **mlc3** treated *Candida* cells with >95% apoptotic cells when treated with $\frac{1}{2}$ MIC values. The other compounds also showed apoptotic activity on *C. albicans* at different ratios when cells were treated with sub-MIC values. At MIC values very, less number (<10%) of apoptotic cells were observed. Cells exposed to positive controls (2 $\mu\text{g}/\text{ml}$ amphotericin B) revealed an increase in TUNEL-positive nuclei identified as green fluorescence spots.

Compounds inducing apoptosis in *Candida* at sub-MIC values is of dominant value as these compounds may then be used for the design of new drugs with fungicidal activity at higher concentrations and programmed cell death at lower concentrations. The most used polyene - amphotericin B, is known to be fungicidal and induces apoptosis in *C. albicans* [22, 23] which could be a possible reason for low resistance levels against this drug. In contrary FLC, which is a fungistatic drug aids *Candida* to develop resistance at lower concentrations [24].

Many metal-based drugs have been demonstrated to show mechanism of action distant from conventional drugs which make them ideal candidates where resistance to conventional drugs has already emerged. The different mechanism of action of metal-based drugs could also be utilized by using them in combination with conventional drugs to target multiple pathways with limited resistance. Some previous studies have shown that treatment of *Candida* with Silver(I) complexes resulted in many morphological features of programmed cell death which was shown to be due to reduction in the ergosterol biosynthesis, a sterol essential to maintain membrane integrity [25]. Altered susceptibility to miconazole and amphotericin B mediated through alterations in the respiration rate has been observed when *Candida* cells were treated with Cu and Ag complexes [26]. In a previous study we observed that treatment of *Candida* with metal complexes disrupts their membrane integrity [20]. In this study we observed that all the metal complexes show synergistic interaction with fluconazole and one of the complexes (**mlc3**) showed

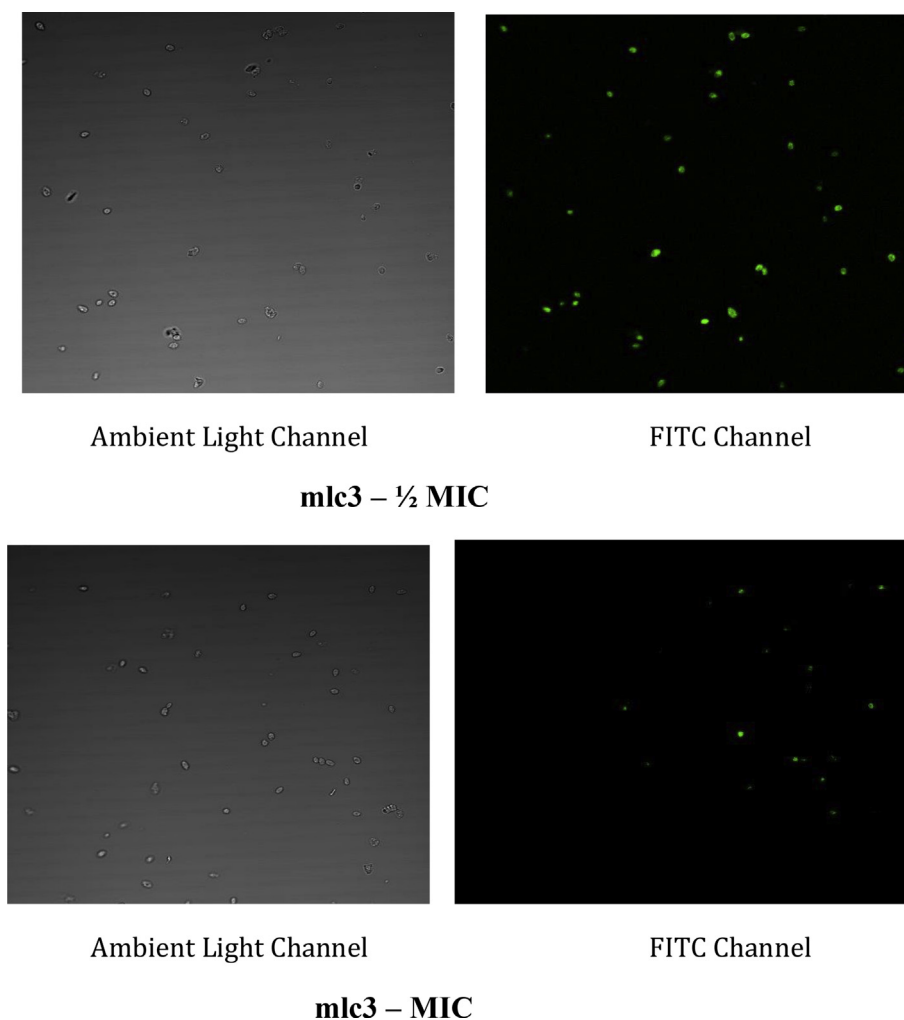


Fig. 5. Fluorescent images of *C. albicans* SC5314 cells treated with MIC and $\frac{1}{2}$ MIC values of *m1c3* complex. Green fluorescence emitting cells are TUNEL-FITC positive, indicating active DNA fragmentation, in cells undergoing apoptosis.

remarkable apoptosis. The different behavior of these otherwise structurally similar complexes could be due to the different nature of the metal ions in their complexes. The most ideal complex (**m1c3**) could be further studied for its detailed mechanism of action by studying the other markers of early and late apoptosis, such as Annexin V-FITC and PI labeling, cytochrome C oxidase activity, membrane potential and ergosterol biosynthesis assay. Furthermore, this complex will also be tested against other species of *Candida* including *C. auris*, which are known multidrug resistant fungal species responsible for several outbreaks worldwide.

3. Conclusions

Isatin and DBM based mixed ligand complexes were synthesized, characterized and evaluated for their antifungal properties. **m1c2** and **m1c3** complexes possess octahedral geometry whereas a distorted octahedral geometry was assigned to the complex **m1c1**, based on various physical and spectroscopic techniques. The biological results revealed that these compounds, with special emphasis to **m1c3**, have a potential to be used as antifungal drugs and significant potentiators with known antifungal azole drug, Fluconazole. The mechanism of action appears to be due to apoptosis in *C. albicans* and therefore this study paves the way for the study and role of metal based drugs as potential antifungal agents and potentiators in mediating fungal cell death by inducing apoptosis. Further investigations would result in a strategy that would lead to the

development of novel antifungal agents that switch on endogenous cell suicide mechanisms and therefore bypasses the development of drug resistance.

4. Experimental

4.1. Materials and physical methods

Isatin, aniline and metal chlorides were analytical grade products from Merck. Dibenzoylmethane was purchased from Aldrich and all chemicals were used as received. Solvents used for the synthesis and analysis was reagent grade chemicals and used without further purification.

The percentages of carbon, hydrogen, nitrogen in Schiff base ligand and metal complexes were determined using Flash EA 1112 elemental analyzer (Thermo Scientific). Electrothermal melting point apparatus was used to determine the melting point of the synthesized compounds. The absorption spectra of the synthesized compounds were recorded between 200-600 nm(cm^{-1}) using UV/visible spectrophotometer (UV-260 Shimadzu, with 1cm quartz cuvettes). IR spectra of the ligand and complexes were recorded in KBr pellets on a Perkin-Elmer 283 spectrophotometer. For ^1H NMR and ^{13}C NMR measurements Bruker WH 300 (200MHz) and Bruker WH 270(67.93 MHz) were used using CDCl_3 or DMSO-d_6 as a solvent and tetramethylsilane as an internal standard. ESI-MS (AB-Sciex 2000, Applied Biosystem) was used to record mass spectra

of the synthesized ligand and complexes. Magnetic moments were measured using Sherwood scientific magnetic susceptibility balance at 25 °C. The thermogravimetric analysis (TGA/DTG) was carried out in the temperature range of 20–1000 °C in a dynamic nitrogen atmosphere with a heating rate of 10 °C/min using NETZSCH STA 449F3 thermal analyzer.

4.2. Synthesis of schiff base ligand and its mixed ligand complexes

4.2.1. Synthesis of 3-(phenylimino)indolin-2-one ligand (L)

To a hot ethanolic solution (20 mL) of isatin (1.47 g, 10 mmol) a 10 mL ethanolic solution of aniline (0.93 g, 10 mmol) was added in the stoichiometric ratio of 1:1 respectively. The reaction mixture was stirred for 5 h at 50 °C and monitored by taking TLC at regular intervals. The resulting clear solution was then reduced to half the volume and then allowed to stay at room temperature. The orange colored crystalline product was then filtered off, washed with least amount of ethanol and diethyl ether several times and then dried in vacuo over CaCl₂ for further use.

Colour (Orange) Yield: 80%. Elemental Anal. Calc. for C₁₄H₁₀N₂O: C, 75.65; H, 4.54; N, 12.61; Found: C, 75.57; H, 4.48; N, 12.65; IR (KBr Pellet, cm⁻¹): 1600 ν(C=N), 1727 ν(C=O), 1340 ν(C-N), 3160 ν(N-H); ¹H NMR (CDCl₃, δ, ppm) 9.46 (s, 1H, NH), 6.65–7.49 (m, 9H, ArH). ¹³C NMR (DMSO-d₆, δ(ppm)): 149.47 (C=O), 163.94 (C=N), 143.43(-C-N=C), 116.15–134.92 (Ar C's), Mass spectrum (ESI) [M + H]⁺ = 223.0. UV-vis (DMSO): λ/nm 255, 305.

4.2.2. Synthesis of mixed ligand complexes

To a 20 mL hot ethanolic solution of dibenzoylmethane (0.45 g, 2 mmol), NaOH (2 mmol) was added. After 15 minutes to the flask was added an ethanolic solution of Schiff base ligand (0.44 g, 2 mmol) and then ethanolic solution of [M(Cl)₂.nH₂O] (2 mmol) was added drop wise with constant stirring. The reaction mixture was refluxed for 5–6 h at 80 °C under nitrogen atmosphere. The reaction mixture was then cooled at room temperature. The product was filtered off, washed several times with ethanol and diethyl ether then dried in vacuum over fused calcium chloride.

[Cu(dbm)LCI(H₂O)]:(mlc1)

Colour (Yellow green) Yield: 70%. Elemental Anal. Calc. for [C₂₉H₂₃ClCuN₂O₄]: C, 61.92; H, 4.12; N, 4.98; Found: C, 60.02; H, 3.97; N, 4.79; IR(KBr Pellet, cm⁻¹): 1543 ν(C=N), 1715 ν(C=O amide), 1620 ν(C=O), 3150 ν(N-H), 3500 ν(OH), 1350 ν(C-N), 1290 ν(C-O), 562 ν(Cu-O), 485 ν(Cu-N); ¹H NMR (DMSO-d₆, δ, ppm) 11.0 (s, 1H, NH), 6.71 (1H, -CH), 3.59 (s, 2H, H₂O), 6.34–8.18 (m, 20H, ArH); ¹³C NMR (DMSO-d₆, δ(ppm)): 150.82 (C=O), 164.75 (C=N), 143.41 (-C-N=C), 93.2 (CH of DBM), 186.8 (C=O of DBM), 183.8 (C-O of DBM), 112.0–133.3 (Ar C's), Mass spectrum (ESI) [M + H]⁺ = 563.50.

[Co(dbm)LCI₂]⁻:(mlc2)

Colour (Brown) Yield: 68%. Elemental Anal. Calc. for [(C₂₉H₂₃Cl₂CoN₂O₃)Na]: C, 60.44; H, 3.85; N, 4.86; Found: C, 60.31; H, 3.87; N, 4.89; IR(KBr Pellet, cm⁻¹): 1586 ν(C=N), 1718 ν(C=O amide), 1640 ν(C=O), 3205 ν(N-H), 1360 ν(C-N), 1290 ν(C-O), 570 ν(Co-O), 486 ν(Co-N); ¹H NMR (DMSO-d₆, δ, ppm) 10.28 (s, 1H, NH), 6.65 (1H, -CH), 6.28–7.52 (m, 19H, ArH). ¹³C NMR (DMSO-d₆, δ(ppm)): 151.15 (C=O), 165.32 (C=N), 138.8 (-C-N=C), 93.7 (CH of DBM), 185.8 (C=O of DBM), 184.8 (C-O of DBM), 112.0–134.1 (Ar C's), Mass spectrum (ESI) [M + H]⁺ = 599.2.

[Ni(dbm)LCI(H₂O)]:(mlc3)

Color (Reddish Brown) Yield: 72%. Elemental Anal. Calc. for [C₂₉H₂₃ClNi₂NiO₄]: C, 62.46; H, 4.15; N, 5.02; Found: C, 61.39; H, 3.98; N, 4.96; IR(KBr Pellet, cm⁻¹): 1580 ν(C=N), 1722 ν(C=O amide), 1648 ν(C=O), 3130 ν(N-H), 3468 ν(OH), 1348 ν(C-N), 1287 ν(C-O), 565 ν(Ni-O), 488 ν(Ni-N); ¹H NMR (DMSO-d₆, δ, ppm) 10.97 (s, 1H, NH),

6.68 (1H, -CH), 3.62 (s, 2H, H₂O), 6.32–7.60 (m, 19H, ArH). ¹³C NMR (DMSO-d₆, δ(ppm)): 151.43 (C=O), 164.92 (C=N), 143.4 (-C-N=C), 93.1 (CH of DBM), 185.2 (C=O of DBM), 182.1 (C-O of DBM), 111.2–130.0 (Ar C's), Mass spectrum (ESI) [M + H]⁺ = 558.70.

4.3. Microbiological analysis

4.3.1. Strains, media and chemicals

In this study, along with one laboratory strain (*Candida albicans* SC5314), three fluconazole (FLC) susceptible (4175; 4179; 4180) and three FLC resistant (4085; 4122; 4135) clinical strains of *C. albicans* were used. Clinical *Candida* strains were isolated from either HIV positive patients or patients with other immunocompromised conditions that were attending clinics at the Charlotte Maxeke Johannesburg Academic Hospital, Johannesburg, South Africa. All the strains were maintained on Sabouraud Dextrose (SD) Agar (Sigma Aldrich, USA) and prior to experiments; cells were grown in fresh SD broth. *Candida albicans* used in this study were isolated from patients under the ethical clearance number M10102 obtained from the Human Research Ethics Committee, University of the Witwatersrand. Fluconazole was purchased from Sigma Fluke (USA) and stock solution of 2 mg/mL was prepared in sterile distilled water. All other chemicals and media were purchased from Sigma Aldrich and Merck.

4.3.2. Determination of Minimum Inhibitory Concentrations and Minimum Fungicidal Concentrations

Minimum Inhibitory Concentrations (MIC) and Minimum Fungicidal Concentrations (MFC) of all the newly synthesized Schiff base ligand and its derivative complexes against all the tested *C. albicans* were determined by a serial dilution technique using Clinical and Laboratory Standards Institute (CLSI) guidelines M27-A3 [27]. Briefly, 100 μL volumes of the test compounds with a final concentration of 2000 μg/mL were added in the first row and were serially diluted. In addition, negative control (1% DMSO), sterility control (media only) and positive control (FLC) were also included in each test. After proper sealing, plates were incubated at 37 °C for 24 h. After incubation, 400 μg/mL of *p*-iodonitrotetrazolium violet solution (INT) was added to each well (40 μL). Viable microorganisms interact with INT to create a colour change from clear to a red-purple colour. Thus, the lowest dilution with no colour change was considered as the MIC for that test compound. Further, MFC was determined by sub-culturing the test dilutions from each well without colour change on SD agar plates and incubated for 24 h. The lowest concentration that showed no fungal growth was defined as the MFC value. All the experiments were done in duplicate and all the results were expressed in μg/mL.

4.3.3. Combination of test compounds with FLC

Based on the MIC values, ligand and its mixed ligand complexes (mlc1–mlc3) were examined for the type of combination interaction with FLC by determining the Fractional Inhibitory Concentration Index (FICI), following the method described previous [28]. In each combination set, test compounds and FLC were added into a well in 1:1 ratio. Interactions were assessed on the basis of zero-interaction theory of Loewe additivity and FICI values were calculated as follows:

$$FICI = FICa + FICb = \frac{MICa \text{ in combination}}{MICa \text{ tested alone}} + \frac{MICb \text{ in combination}}{MICb \text{ tested alone}}$$

where MICa is the MIC of the Schiff base derivatives and MICb is the MIC of drug (FLC). Interpretations of FICI values were done as synergy when ≤0.5, additive between 0.5 and 1.0, indifferent between 1.0 and 4.0 and antagonistic when FICI values were >4.0.

4.3.4. Apoptosis study

To study the apoptotic effect of ligand and its mixed ligand complexes (mlc1–mlc3) against *C. albicans*, Terminal deoxynucleotidyl transferase-mediated dUTP nick end labeling (TUNEL) assay was

performed by using *In Situ* Cell Death Detection Kit, Fluorescein (Roche Applied Science), as described previously [29]. Briefly, cells were exposed to MIC and ½ MIC values of all the test compounds followed by washing 3 times in PBS. Cells are then fixed with a fixative solution (4% paraformaldehyde in PBS pH 7.4) for 1 hour at 25 °C. After fixation protoplasts were prepared by digesting cell wall with lyticase in different washing steps in protoplast buffers pH 7.4 (buffer I - containing 1M sorbitol, 50 mM tris base, 10 mM MgCl₂ and 30 mM DTT; buffer II – 1M sorbitol, 50 mM tris base, 10 mM MgCl₂ and 1 mM DTT; buffer III – 1M sorbitol, 50 mM tris base and 10 mM MgCl₂). Cells were harvested and washed thrice for 5 min each with buffer I (3 mL/g cells). Cells were then incubated in buffer II (5 mL/g cells; supplemented with lyticase) for 2 h at 25 °C. Centrifuge and discard the supernatant then incubated with buffer III (5 mL/g cells) for 20 min. Again, centrifuge to remove buffer III, then washed the protoplasts once with PBS and incubated with permeabilization solution (0.1% Triton X-100 in 0.1% sodium citrate) for 2 min on ice, then again rinsed twice with PBS. Stain with 50 µL TUNEL reaction mixture and incubate for 60 min at 37 °C in a humidified atmosphere in the dark. Wash cells twice with PBS and examine by fluorescent microscope (Zeiss LSM 780 - laser scanning confocal microscope) with an excitation wavelength of 488 nm and the detection range of 515 nm. Two negative controls and a positive control should be run with each experiment.

Declarations

Author contribution statement

Mohammad Younus Wani: Conceived and designed the experiments; Analyzed and interpreted the data; Wrote the paper.

Ovas Dar, Faisal Mohammed Aqlan: Performed the experiments; Analyzed and interpreted the data; Wrote the paper.

Shabir Lone: Performed the experiments.

Manzoor Malik: Performed the experiments; Analyzed and interpreted the data.

Athar Hashmi: Contributed reagents, materials, analysis tools or data.

Aijaz Ahmad: Conceived and designed the experiments; Analyzed and interpreted the data; Contributed reagents, materials, analysis tools or data; Wrote the paper.

Funding statement

This research did not receive any specific grant from funding agencies in the public, commercial, or not-for-profit sectors.

Competing interest statement

The authors declare no conflict of interest.

Additional information

Supplementary content related to this article has been published online at <https://doi.org/10.1016/j.heliyon.2019.e02055>.

References

- [1] M.E. Katsarou, E.K. Eftimiadou, G. Psomas, A. Karaliota, D. Vourloumis, Novel copper(II) complex of N-propyl-norfloxacin and 1,10-phenanthroline with enhanced antileukemic and DNA nuclease activities, *J. Med. Chem.* 51 (2008) 470–478.
- [2] W. Guerra, E. de Andrade Azevedo, A.R. de Souza Monteiro, M. Bucciarelli-Rodriguez, E. Chartone-Souza, A.M.A. Nascimento, A.P.S. Fontes, L. Le Moyec, E.C. Pereira-Maia, Synthesis, characterization, and antibacterial activity of three palladium(II) complexes of tetracyclines, *J. Inorg. Biochem.* 99 (2005) 2348–2354.
- [3] I. Turel, L. Golic, P. Bukovec, M. Gubina, Antibacterial tests of Bismuth(III)–Quinolone (Ciprofloxacin, cf) compounds against *Helicobacter pylori* and some other bacteria. Crystal structure of (cH₂)₂[Bi₂Cl₁₀]·4H₂O, *J. Inorg. Biochem.* 71 (1998) 53–60.
- [4] G.S. Singh, Z.Y. Desta, Isatins as privileged molecules in design and synthesis of spiro-fused cyclic frameworks, *Chem. Rev.* 112 (2012) 6104–6155.
- [5] H. Pervez, M. Ahmad, S. Zaib, M. Yaqub, M.M. Naseer, J. Iqbal, Synthesis, cytotoxic and urease inhibitory activities of some novel isatin-derived bis-Schiff bases and their copper(II) complexes, *Medchemcomm* 7 (2016) 914–923.
- [6] P. Davidovich, V. Aksenova, V. Petrova, D. Tentler, D. Orlova, S. Smirnov, V. Gurzhiiy, A.L. Okorokov, A. Garabadzhiu, G. Melino, N. Barlev, V. Tribulovich, Discovery of novel isatin-based p53 inducers, *ACS Med. Chem. Lett.* 6 (2015) 856–860.
- [7] H. Torres-Gomez, E. Hernandez-Nunez, I. Leon-Rivera, J. Guerrero-Alvarez, R. Cedillo-Rivera, R. Moo-Puc, R. Argotte-Ramos, M. del Carmen Rodriguez-Gutiérrez, M.J. Chan-Bacab, G. Navarrete-Vazquez, Design, synthesis and in vitro antiprotozoal activity of benzimidazole-pentamidine hybrids, *Bioorg. Med. Chem. Lett.* 18 (2008) 3147–3151.
- [8] E.F. Canzi, F.M. dos Santos, E.K. Meneghetti, B.H.L.N. Sales Maia, J.M. Batista, Absolute configuration of a rare dibenzoylmethane derivative from *dahlstedtia glaziovii* (Fabaceae), *Tetrahedron Lett.* 59 (2018) 135–137.
- [9] M.L. Daly, C. Kerr, C.A. DeRosa, C.L. Fraser, Meta-alkoxy-substituted difluoroboron dibenzoylmethane complexes as environment-sensitive materials, *ACS Appl. Mater. Interfaces* 9 (2017) 32008–32017.
- [10] W.H. Mahmoud, G.G. Mohamed, O.Y. El-Sayed, Coordination compounds of some transition metal ions with new Schiff base ligand derived from dibenzoyl methane. Structural characterization, thermal behavior, molecular structure, antimicrobial, anticancer activity and molecular docking studies, *Appl. Organomet. Chem.* 32 (2018) e4051.
- [11] M. Halliday, H. Radford, K.A.M. Zents, C. Molloy, J.A. Moreno, N.C. Verity, E. Smith, C.A. Ortori, D.A. Barrett, M. Bushell, G.R. Mallucci, Repurposed drugs targeting eIF2α-P-mediated translational repression prevent neurodegeneration in mice, *Brain* 140 (2017) 1768–1783.
- [12] M.A. Malik, O.A. Dar, P. Gull, M.Y. Wani, A.A. Hashmi, Heterocyclic Schiff base transition metal complexes in antimicrobial and anticancer chemotherapy, *Medchemcomm* 9 (2018) 409–436.
- [13] M.Y. Wani, A. Ahmad, S. Kumar, A.J.F.N. Sobral, Flucytosine analogues obtained through Biginelli reaction as efficient combinative antifungal agents, *Microb. Pathog.* 105 (2017) 57–62.
- [14] A. Ahmad, M.Y. Wani, M. Patel, A.J.F.N. Sobral, A.G. Duse, F.M. Aqlan, A.S. Al-Bogami, Synergistic antifungal effect of cyclized chalcone derivatives and fluconazole against *Candida albicans*, *Medchemcomm* 8 (2017) 2195–2207.
- [15] M.A. Ali, H.J. HJ Abu Bakar, A.H. Mirza, S.J. Smith, L.R. Gahan, P.V. Bernhardt, Preparation, spectroscopic characterization and X-ray crystal and molecular structures of nickel(II), copper(II) and zinc(II) complexes of the Schiff base formed from isatin and S-methylthiocarbamate (Hisa-sme), *Polyhedron* 27 (2008) 71–79.
- [16] A.S. El-Tabl, F.A. El-Saied, W. Plass, A.N. Al-Hakimi, Synthesis, spectroscopic characterization and biological activity of the metal complexes of the Schiff base derived from phenylaminoacetohydrazide and dibenzoylmethane, *Spectrochim. Acta Part A Mol. Biomol. Spectrosc.* 71 (2008) 90–99.
- [17] G.Y. Nagesh, K. Mahendra Raj, B.H.M. Mruthyunjayaswamy, Synthesis, characterization, thermal study and biological evaluation of Cu(II), Co(II), Ni(II) and Zn(II) complexes of Schiff base ligand containing thiazole moiety, *J. Mol. Struct.* 1079 (2015) 423–432.
- [18] P. Wayne, Clinical and Laboratory Standards Institute: Reference Method for Broth Dilution Antifungal Susceptibility Testing of Yeasts; Fourth Informational Supplement, 2012 (Document M27-S4).
- [19] S.K. Shrestha, M.Y. Fosso, S. Garneau-Tsodikova, A combination approach to treating fungal infections, *Sci. Rep.* 5 (2015) 17070.
- [20] M.Y. Wani, A. Ahmad, M.A. Malik, A.J.F.N. Sobral, Mononuclear transition metal complexes containing iodo-imidazole ring endowed with potential anti-Candida activity, *Med. Chem. Res.* 25 (2016) 2557–2566.
- [21] D. Carmona-Gutierrez, T. Eisenberg, S. Büttner, C. Meisinger, G. Kroemer, F. Madeo, Apoptosis in yeast: triggers, pathways, subroutines, *Cell Death Differ.* 17 (2010) 763–773.
- [22] R.S. Al-Dhaheri, L.J. Douglas, Apoptosis in *Candida* biofilms exposed to amphotericin B, *J. Med. Microbiol.* 59 (2010) 149–157.
- [23] A.J. Phillips, I. Sudbery, M. Ramsdale, Apoptosis induced by environmental stresses and amphotericin B in *Candida albicans*, *Proc. Natl. Acad. Sci.* 100 (2003) 14327–14332.
- [24] D.M. Arana, C. Nombela, J. Pla, Fluconazole at subinhibitory concentrations induces the oxidative- and nitrosative-responsive genes TRR1, GRE2 and YHB1, and enhances the resistance of *Candida albicans* to phagocytes, *J. Antimicrob. Chemother.* 65 (2010) 54–62.
- [25] B. Thati, A. Noble, R. Rowan, B.S. Creaven, M. Walsh, M. McCann, D. Egan, K. Kavanagh, Mechanism of action of coumarin and silver(I)–coumarin complexes against the pathogenic yeast *Candida albicans*, *Toxicol. In Vitro* 21 (2007) 801–808.
- [26] A. Eshwika, B. Coyle, M. Devereux, M. McCann, K. Kavanagh, Metal complexes of 1,10-phenanthroline-5,6-dione alter the susceptibility of the yeast *Candida albicans* to Amphotericin B and Miconazole, *BioMetals* 17 (2004) 415–422.
- [27] P. Wayne, Clinical and Laboratory Standards Institute: Reference Method for Broth Dilution Antifungal Susceptibility Testing of Yeasts; Approved Standard, 2008, p. 3. CLSI document M27-A3 and Supplement S.
- [28] A. Ahmad, M.Y. Wani, A. Khan, N. Manzoor, J. Molepo, Synergistic interactions of Eugenol-tosylate and its congeners with fluconazole against *Candida albicans*, *Plos one* 10 (2015) e0145053.
- [29] A. Kha, n. A. Ahmad, L.A. Khan, N. Manzoor, Ocimum sanctum (L.) essential oil and its lead molecules induce apoptosis in *Candida albicans*, *Res. Microbiol.* 165 (2014) 411–419.